Beat-Wave Excitation of Plasma Wave and Observation of Accelerated Electrons

Y. Kitagawa, T. Matsumoto, T. Minamihata, K. Sawai, K. Matsuo, K. Mima, K. Nishihara, H. Azechi, K. A. Tanaka, H. Takabe, and S. Nakai

Institute of Laser Engineering, Osaka University, Suita, Osaka, 565, Japan

(Received 12 March 1990)

The simultaneous observations of a beat-wave-excited plasma wave and of energetic electrons are reported. A plasma wave is excited when the beat-wave frequency of a laser with two wavelengths 10.6 and 9.57 μm equals the plasma frequency. The Stokes sideband measurement gives a wave amplitude $\delta n/n_0$ of $\sim 5\%$. Plasma electrons with the energies of more than 10 MeV are observed at the resonant density.

PACS numbers: 52.35.Fp, 52.35.Mw, 52.90.+z

Since Tajima and Dawson proposed the laser beat-wave accelerator as a promising collective acceleration scheme [1], there have been many theoretical studies [2–5], in view of the number of potentially important applications in the fields of plasma physics, astrophysics, and particle accelerator physics, but only a few experimental studies. Clayton *et al.* first demonstrated plasma-wave excitation by a resonant laser beat wave [6], and this was followed by the work of Ebrahim *et al.* [7]. Other work of Ebrahim *et al.* suggested beat-wave-accelerated electrons [8]. In this Letter, we present the simultaneous observations of a 10.6- and 9.57-μm beat-wave-excited plasma wave and of electrons with energies of more than 10 MeV. The electric field of the wave is more than 1 GV/m. The observed energetic electrons support the possibility that a beat-wave accelerator mechanism may have been operative, but the maximum energies observed exceed predicted values by factors of 2–4.

A schematic of the apparatus is shown in Fig. 1. A double-line CO_2 laser beam comes from the LEKKO VIII electron-beam-controlled laser system [9]. A cw oscillator injects a 9.569-μm line to the oscillator cavity. The system then produces a pulse of 0.4-ns rise time and 1-ns full width at half maximum containing 150 J each in the 10.591-μm [10p(20)] and 9.569-μm [9P(22)] lines. An $f/10$ NaCl lens focuses the laser beam from 23 cm diam to a spot of less than 1 mm, resulting in an intensity $I \geq 2\times10^{13}$ W/cm^2 for each line. The absolute intensity will be between 2×10^{13} and 2×10^{14} W/cm^2 [10]. At the focal point in the vacuum chamber, an electromagnetically driven gas puff injects hydrogen gas 300 μs prior to the laser irradiation, which produces a hydrogen plasma. By controlling gas flows, we could change the electron density n_0 at the focal point from 3×10^{16} to 7×10^{17}/cm^3 within 30% error [11]. The beat-wave frequency between 10.6 and 9.57 μm equals the plasma frequency corresponding to 1.1×10^{17}/cm^3. From the Stark broadening measurement of the hydrogen Balmer-α line (6562.8 Å) emission we estimated the electron density. 8.5 Å full width at half power corresponds to 1.1×10^{17}/cm^3 for an electron temperature of > 10 eV [12]. The spectral resolution is 1 Å, i.e., 1×10^{16}/cm^3. The measurement of the Balmer-α line emission area shows that the plasma is cylindrical with a diameter of 1.8 mm and an axial length of 7 mm. A time-resolved measurement shows the density is constant in ~ 5 ns from the laser onset [11]. In the present experiment we injected no electrons and so we did not drive the solenoid coil in the chamber.

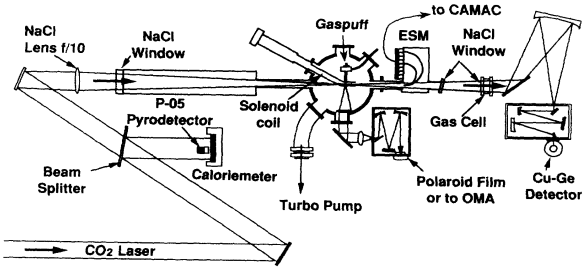

FIG. 1. Experimental setup for the beat-wave acceleration.

The double-line laser beam, as soon as it produces the resonant density plasma, excites the plasma wave in it. The ratio of the laser frequency to the plasma frequency, γ_p, is 10. The excited plasma wave in turn forward scatters the pump waves to Stokes (11.857 μm) and anti-Stokes (8.7 μm) sidebands and probably also to their harmonic series. The Stokes line intensity P_s is expressed by the Bragg scattering formula as [13]

$$\frac{P_s}{P_0} = \left[\frac{\pi}{2}\frac{\delta n}{n_0}\frac{n_0}{n_c}\frac{L}{\lambda_0}\right]^2, \quad (1)$$

where P_0 is the 10.6-μm pump intensity, δn is the electron density perturbation, n_c is the cutoff density, and L and λ_0 are the length of the excited plasma wave and the laser wavelength. We measured P_s and P_0 using a monochrometer with a liquid-helium–cooled Cu-Ge detector to confirm the plasma wave excitation and to estimate its amplitude $\delta n/n_0$. The detector sensitivity is almost constant over the frequency range from 10.6 to 11.86 μm. The signal ratio P_s/P_0 was expected to be very small and indeed was from 0.001 to 0.08, so that to detect P_s we had to put a gas cell in the light path, as shown in Fig. 1. The cell, containing a 100-Torr mixture of SF_6 and C_2F_3Cl, absorbed 99.9% of the 10.6-μm and 94% of the 9.57-μm pumps, preventing damage of the monochroma-

tor optics as well as suppressing the stray signal level to less than $0.001P_0$. To detect P_0 and thus to obtain an absolute ratio of P_s/P_0, we replaced the cell with Teflon foil attenuators. The attenuation includes $\pm 25\%$ error. The pulse rise and width of the Stokes line P_s and thus of the plasma wave agreed with those of P_0 within the detector-scope (Tektronix 7104) response time of < 1 ns. P_0 was also measured by a P-05 pyroelectric detector.

In Fig. 2 are Stokes signals P_s/P_0 as a function of n_0. They show a peak of 0.05 at $1.4\times10^{17}/\text{cm}^3$ and a broad resonance feature from 0.7 to $3\times10^{17}/\text{cm}^3$. The stray light (noise) level is about 0.001. The reason why it is so broad is that, whenever n_0 is higher than the resonant density, either the front or the rear of the focal point should satisfy the resonant condition to excite the wave. The vertical bars in the figure show the P_0 calibration error of 25%. From Eq. (1) the amplitude $\varepsilon=\delta n/n_0$, giving $P_s/P_0=0.05$ (0.007–0.06), is $\sim5\%$ (2%–6%) supposing $L=3$ mm. Since we have not directly measured L, we assumed L to equal the electron-ion collision mean free path. The mean free path is 3 mm, or the mean free time is 10 ps, for the electron temperature of 100 eV. The mean free path is roughly the homogeneous length out of the 7-mm plasma. Under the present conditions the saturation amplitude ε_s due to relativistic frequency shift predicted by Rosenbluth and Liu [14] is $[\frac{16}{3}(eE_0/m\omega_0 c)eE_1/m\omega_1 c]^{1/3}\approx 20\%$, where (E_0,ω_0) and (E_1,ω_1) denote the electric field and frequency of the 10.6- and 9.57-μm lines, respectively. This value is 4 times that obtained above, $\varepsilon=5\%$ (the wave field of 1.5 GV/m). Even for the single-line irradiation, we detected small but not stray signals at 11.857 μm around $10^{17}/\text{cm}^3$. They are shown by open circles in the figure, corresponding to $\varepsilon\sim1\%$. They may be due to instabilities such as a forward Raman scattering (FRS), since, when the intensity is 10^{14} W/cm^2, it is on the threshold level for FRS [15,16].

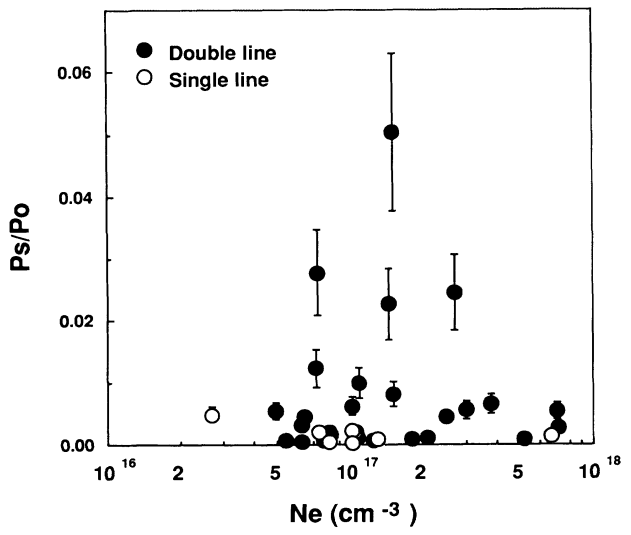

FIG. 2. Forward-scattered Stokes sideband intensity P_s at 11.857 μm divided by 10.6-μm pump intensity P_0 plotted as a function of the electron density: Solid circles are for double-line and open circles for single-line irradiation. Vertical bars denote P_0 calibration error of 25%. The detection limit is 0.001.

The plasma wave with ε and γ_p can trap and accelerate either plasma electrons or injected electrons, having initial kinetic energies $(\gamma'-1)mc^2$, as long as $(\gamma'-1)mc^2 < \varepsilon\gamma_p mc^2$ is fulfilled. Thus, in the laboratory frame, the electrons having kinetic energy not less than

$$W_{\min}=mc^2[\gamma_p(\gamma_p\varepsilon+1)(1-\beta_p\beta')-1] \quad (2)$$

are accelerated to final energies of

$$W_{\max}=mc^2[\gamma_p(\gamma_p\varepsilon+1)(1+\beta_p\beta')-1], \quad (3)$$

where $\beta_p=(1-1/\gamma_p^2)^{1/2}$ and $\beta'=[1-1/(\gamma_p\varepsilon+1)^2]^{1/2}$. Here γ' and β' are the wave-frame quantities of electrons [11]. Equations (2) and (3) show that the plasma wave of $\varepsilon=5\%$ accelerates 1.4-MeV electrons to 12 MeV over a distance of 7 mm. The energy gain is more than 10 MeV.

An eight-channel electron spectrometer (ESM) placed at 85 cm from the focal point covers electron energies from 2.5 to 21 MeV. A permanent dipole magnet of 5 kG bends electrons by 180°. The entrance aperture is 8 mm in diameter, i.e., 7×10^{-5} sr. Each channel, whose window width is 0.6 MeV, has a plastic scintillator (Pilot-U; $\frac{1}{2}$ in. diam and 4 cm long)—photomultiplier coupling linked to a CAMAC. By using 18- to 20-MeV rf linac electron beams, we have calibrated the energies and sensitivities of the ESM channels [11]. An electron of 20 MeV entering the window yields about 1×10^7 electrons out of the photomultiplier. The sensitivities of 2- to 18-MeV channels are calculated in proportion to energy. We have also used 3-MeV electron beams from an induction linac. Figure 3(a) shows the number of electrons injected into the ESM channel windows from the plasma with double-line irradiation. Identical symbols correspond to the same shot. The large symbols are for the resonant condition $[(1-2)\times10^{17}/\text{cm}^3]$ and the small ones are for off resonance. The parameters on the right-hand side show (incident laser energy)/(electron density). To know the noise level or the detection limit, we put a deflecting dipole magnet of 0.7 kG in front of the ESM aperture, which shows the noise level as ~10 electrons/channel, although somewhat different for each channel. The electron spectra seem to have two components, i.e., low-energy (less than ~10 MeV) and high-energy tail (more than 10 MeV) components, especially for the resonant density shots. With single-line irradiation at resonance, as seen in Fig. 3(b), the spectra seem not to have such high tails.

We summed up the number of the low-energy (2.5 to 8 MeV) and high-energy (10 to 21 MeV) components separately and plotted them as a function of the electron density. Thus, we found that with double-line irradiation,

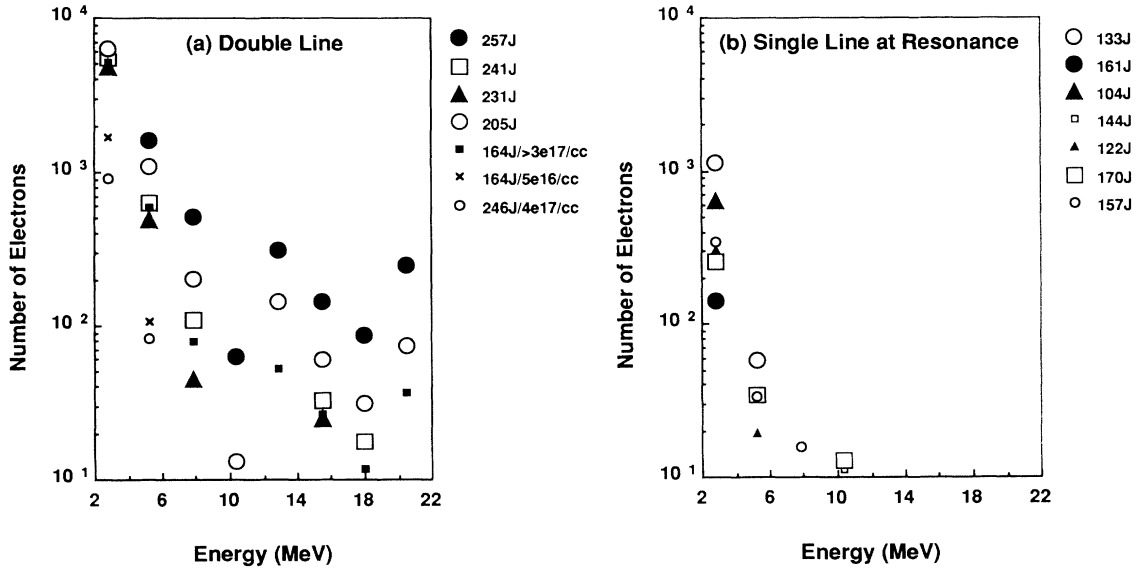

FIG. 3. Energy spectra of the electrons forward emitted from the hydrogen plasma and analyzed with an electron spectrometer (ESM). Number of electrons per channel (a) with double-line irradiation both at and off resonance and (b) with single-line irradiation at resonance [$(1-2)\times10^{17}/\mathrm{cm}^3$]. Identical symbols are from the same shot, of which the parameter is (laser energy)/n_0. Noise level is ~ 10 electrons.

the high-energy components have a resonant peak in the density, though there is some data scattering, while the low-energy components show not a sharp, but rather a broad (weak resonant) feature [see Figs. 4(a) and 4(b)]. The vertical error bar is, then, ± 50 electrons and the horizontal bar is the density measurement error. It seems that the low-energy electrons are accelerated to 10 MeV or more by the beat-wave-excited plasma wave. It is, however, not consistent with an ε of $\sim 5\%$, because most of the high-energy components are too high to be accelerated by one wave. 1.5 GV/m (5%) times 3 mm only provides 4.5 MV. If we suppose an amplitude of 6% and an acceleration distance of 7 mm, which is the plasma length, the gain becomes 14 MeV, but the distance is twice the length of the plasma wave. This is not yet understood. It may be explained by multiple-stage accelera-

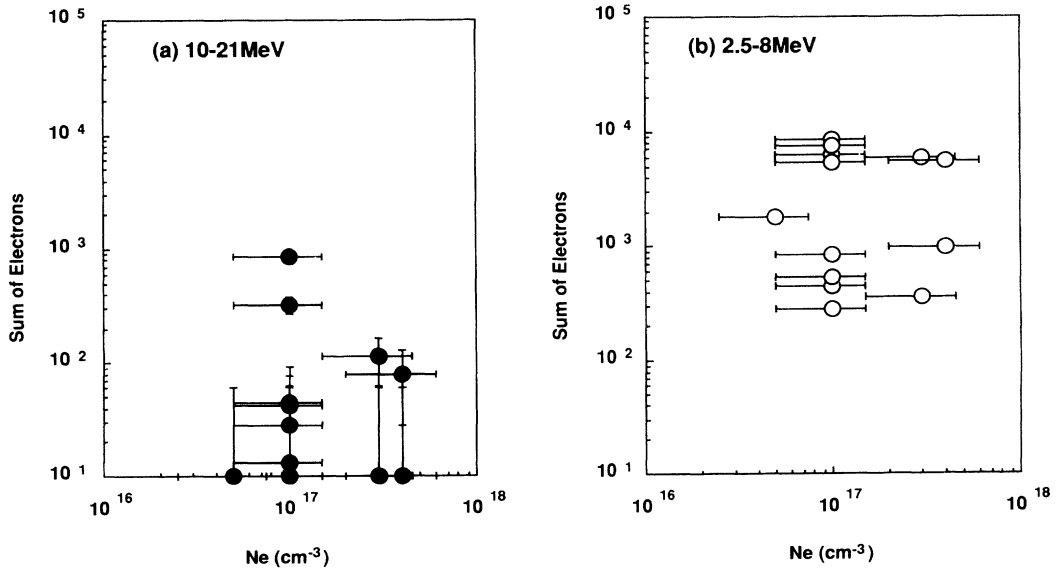

FIG. 4. (a) Number of the high-energy electrons summed over the ESM channels (10–21 MeV) vs the electron density with double-line irradiation. (b) Number of the low-energy electrons (2.5–8 MeV). Vertical error bar is 50 electrons. Horizontal error bar is the density measurement error.

tion, for instance [17]. However, even this does not account for the data between 14 and 21 MeV.

It is plausible that the low-energy components are trapped by the wave potential, since their broad resonant feature suggests that the beat wave would also affect them [see Fig. 4(b)]. However, the reason for emission of the low-energy components for both single- and double-line irradiations is, as well, not clear. Even if forward Raman scattering of $\varepsilon \sim 1\%$ is excited, the trapping threshold for a 1% FRS wave is too high (~ 3 MeV) to trap thermal plasma electrons, and the FRS amplitude (~ 0.3 GV/m) is too low to account for the observed 2.5–8-MeV electrons.

The FRS might Landau damp the excited plasma wave to limit the wave amplitude to a few percent. Whenever stimulated Raman scattering such as the FRS is excited, stimulated Brillouin scattering could also invariably be excited, which may cause plasma rippling to limit the effective length of the plasma wave to several mm [18].

In Figs. 2 and 4, the resonant density seems to be not 1.1×10^{127} but $1.4\times10^{17}/\mathrm{cm}^3$. So, the absolute density may need correction by a factor of 1.2.

In summary we simultaneously observed a beat-wave-excited plasma wave and energetic electrons. The 10.6- and 9.57-μm beat wave excited a plasma wave of $\varepsilon \sim 5\%$ at resonant density. The field is ~ 1.5 GV/m. We observed, then, plasma electrons with the energies of ~ 10 MeV or more. The observed energetic electrons support the possibility that a beat-wave accelerator mechanism may have been operative, but the maximum energies observed exceed predicted values by factors of 2–4.

We thank C. Yamanaka for his encouragement, and S. Nakayama for making the ESM. Also we thank S. Goto of the Plasma Physics Laboratory, Osaka University for preparing the gas puff and K. Tsumori of the Radiation Laboratory, the Institute of Science and Industrial Research, Osaka University for the ESM calibration. One of the authors, Y. Kitagawa, acknowledges useful discussions with F. F. Chen, C. Joshi, and their UCLA group.

[1] T. Tajima and J. M. Dawson, Phys. Rev. Lett. **43**, 267 (1979).
[2] T. Katsouleas and J. M. Dawson, Phys. Rev. Lett. **51**, 392 (1983).
[3] D. W. Forslund and J. M. Kindel, Phys. Rev. Lett. **54**, 558 (1985).
[4] C. Darrow *et al.*, Phys. Rev. Lett. **56**, 2629 (1986).
[5] K. Mima *et al.*, Phys. Rev. Lett. **57**, 1421 (1986).
[6] C. E. Clayton *et al.*, Phys. Rev. Lett. **54**, 2343 (1985).
[7] N. A. Ebrahim *et al.*, in *Proceedings of the 1986 Linear Accelerator Conference, Stanford, California* (SLAC Report No. 303, 1986), p. 552.
[8] N. A. Ebrahim *et al.*, IEEE Trans. Nucl. Sci. **32**, 3539 (1985).
[9] C. Yamanaka *et al.*, IEEE J. Quantum Electron. **17**, 1678 (1981).
[10] K. Terai *et al.*, Rev. Laser Eng. **12**, 37 (1984) (in Japanese).
[11] Y. Kitagawa *et al.*, Quarterly Progress Report, Institute of Laser Engineering, Osaka University, Report No. ILE-QPR-91-39, 1992 (to be published).
[12] C. Bekefi, *Principle of Laser Plasmas* (Wiley, New York, 1976), Chap. 13.
[13] R. E. Slusher and C. M. Surko, Phys. Fluids **23**, 472 (1980).
[14] M. N. Rosenbluth and C. S. Liu, Phys. Rev. Lett. **29**, 701 (1972).
[15] K. Estabrook and W. L. Kruer, Phys. Fluids **26**, 1892 (1983).
[16] C. Joshi *et al.*, Phys. Rev. Lett. **47**, 1285 (1981).
[17] T. Tajima, Laser Particle Beams **3**, 351 (1985).
[18] K. Mima and K. Nishikawa, in *Basic Plasma Physics II*, edited by A. A. Galeev and R. N. Sudan (North-Holland, Amsterdam, 1984), Chap. 6.5.